LIMNOLOGY
and
OCEANOGRAPHY: METHODS

Limnol. Oceanogr.: Methods 3, 2005, 10–23

High-resolution permeability determination and two-dimensional porewater flow in sandy sediment

Carlos Rocha[1], Stefan Forster[2], Erica Koning[3], and Eric Epping[3]*

[1]Center for Marine and Environmental Research (CIMA), Faculdade de Ciências do Mar e Ambiente (FCMA), Universidade do Algarve, Campus de Gambelas, 8000-810 Faro, Portugal

[2]Institute for Biological Sciences - Marine Biology, Albert-Einstein-Strasse 3, D18051 Rostock, Germany

[3]Royal Netherlands Institute for Sea Research (Royal NIOZ), Department of Marine Chemistry and Geology, Texel, The Netherlands

Abstract

A new, inexpensive method is proposed to measure permeability in natural sandy sediment with high spatial resolution. This methodology allows for a reconstruction of the vertical permeability anisotropy in natural sediments, with a depth resolution of a few millimeters. Thus, the possible intrusion depth of advective flow over the water-sediment interface of sandy sediments can be deduced. Shipboard measurements on five natural sandy sediment cores taken from North Sea sediments are used to demonstrate that both the direction and magnitude of the second-order permeability tensor can be calculated from direct measurements using this method. This presents a major improvement over previous methods particularly in the context of quantifying flow and reaction in permeable sediments.

Recent evidence suggests that the sandy, permeable seabed is at least as important in biogeochemical cycling of organic matter as muddy, cohesive sediments (*see* overview by Boudreau et al. 2001). Low-standing stock of organics and inorganic byproducts of diagenesis found in permeable sediments, as opposed to larger reservoirs located in cohesive sediments, are now being explained, not as a reflection of low biogeochemical activity, but instead by rapid turnover, aided by advective interfacial flow (Rocha 2000 1998; Huettel et al. 1998, Huettel et al. 1996; Shum and Sundby 1996; Webster et al. 1996; Thibodeaux and Boyle 1987; Webb and Theodor 1968). A description of flow within the sedimentary matrix near the sediment-water interface is now needed to update diagenetic models describing biogeochemical fluxes and reaction kinetics in sandy sediments. Coupling of transport processes to the geochemical 2-d and 3-d zonation found in the rippled sea bottom will be crucial to understanding the contribution of coastal and shelf sands to the overall carbon budget (Boudreau et al. 2001). However, it is first necessary to understand the factors that affect the magnitude and vertical penetration of advective flow in sandbeds.

Quantification of boundary layer flow penetration into a permeable medium is a complex physical challenge that has been examined through a variety of different approaches in the context of oxygen transport through the sediment-water interface (Huettel et al. 1998; Güss 1998; Lohse et al. 1996; Booij et al. 1991; Svensson and Rahm 1991). Extent of porewater flow is controlled by permeability of the medium and by magnitude of the horizontal pressure gradient driving the flow (Dullien 1992; Darcy 1856). From experimental observations in laboratory flume studies, significant porewater flow in sediments seems to occur only above a cut-off bulk permeability of circa 10^{-12} m^2 (Huettel and Gust 1992), as measured by classical approaches of constant or falling head permeametry (Klute and Dirksen 1986; Klute 1965). Boundary layer flow is linked to Darcian flow within the sediment by a transitional layer called the Brinkman layer (Brinkman 1947). The width

*E-mail: crocha@ualg.pt

Acknowledgments

This paper is dedicated to the memory of Dr. Wim van Raaphorst. He is gratefully acknowledged for providing an inspiring environment where the free interchange of scientific ideas around the theme was crucial for the accomplishment of this work. His passing away before the end of this project has left a deep sense of tragedy within the research team. This study was supported by Project EMIR (Enhanced organic carbon mineralization rates in permeable sandy sediments) and hosted by the Royal Netherlands Institute for Sea Research (NIOZ). The authors also wish to thank the captain and crew of the R.V. *Pelagia* for providing a safe journey and for assistance onboard. CR was jointly funded by the Portuguese National Foundation for Science and Technology (FCT) through contract SFRH/BPD/6042/2001, NIOZ, and the Centre for Marine and Environmental Research (CIMA). We would also like to thank *Limnology & Oceanography: Methods* associate editor, Prof. David Thistle, and two anonymous reviewers for comments and suggestions that clearly improved the original manuscript.

of the Brinkman layer has been put at approximately the square root of permeability of the porous medium, which, in general, corresponds to grain-size scale (Boudreau 1997). However, observed patterns of interstitial advective flow near a porous bed-water interface caused by overlying shear have been observed to clearly surpass this empirical barrier (Güss 1998), putting the measurable penetration depth at 20 to 100 times the square root of permeability (Gupte and Advani 1997). It is then clear that further development of this concept is needed, aiming to quantify porewater exchange in natural sediment beds subject to hydrodynamic shear stress.

Permeability may change with direction inside the sediment and depends on its heterogeneity. Isotropic porous media (permeability is equal in all directions inside a sample volume) is a theoretical assumption used to simplify solutions of the governing equations for flow in porous media, both on large-scale hydrology (Dullien 1992) and comparatively small scale flow through permeable sediments (Huettel et al. 1998). However, natural sediments are mostly anisotropic, meaning that the vertical hydraulic conductivity (K_v) is different from the horizontal hydraulic conductivity (K_h). Heterogeneity is where the hydraulic conductivity in one place differs from that measured in another. In natural soils and sediments, both anisotropy and spatial heterogeneity exist, affecting both the pattern and rates of interstitial water flow (Dullien 1992; Dagan 1984; Freeze and Cherry 1979).

Laboratory investigations of permeability are made on volumes of about 20 cm^3. Conversely, field measurements in catchment areas are based on well log data pertaining to volumes on the order of 20,000 cm^3 (Haldorsen 1986). So, although detailed information might be available on small sampled volumes of soil, the spatial distribution of the permeability at basin scale can only be extracted as an equivalent or "lumped" value. Thus, a change in scale through several orders of magnitude in length is necessary to achieve mapping of K at basin scales (Vogel and Roth 2003). Consequently, mapping of flow at basin scale will necessarily be hampered by the absence of detailed information on the spatial distribution of permeability (heterogeneity) as well as its directional behavior (anisotropy). This upscaling problem, as yet not solved satisfactorily, remains a source of a lot of research (*see* review by Renard and Marsily 1997, and references therein). The main difficulty is that hydraulic conductivity is not an additive variable: it is impossible to calculate equivalent permeability by simple arithmetic average (*see* Renard et al. 2000). So, regular interpolation for missing values of K at large scales is not possible. However, what is pertinent to recent literature on advective porewater flow and biogeochemistry of marine sediments (Reimers et al. 2004; Huettel et al. 1998) is the converse problem of downscaling. The question of how small-scale water flows develop at the very surface (few mm^2) of natural sediments is crucial to model reaction and compound residence time. Here, sediment has been assumed isotropic on a scale larger than the scale of interest.

On the contrary, real macroscopic media, such as natural marine sediments, are anisotropic because of compaction, sedimentation layering, and ripple migration (Dullien 1992; Phillips 1991). Resuspension events also contribute to decrease cohesiveness of the very top of the sediment surface. In other words, permeability measurements for a 15-cm long sediment core will not apply to smaller scales of interest, such as the benthic oxic layer, often limited to a few millimeters. This has implications, for instance, on the parameterization of the mixing depth for oxygen in natural sandy sediments subject to boundary layer flow. In addition, the method for bulk permeability measurement generally applied in benthic mineralization studies does not allow quantification of the permeability anisotropy of the sediment. This is, however, required to identify the depth range of interstitial flow through the water-sediment boundary layer and to couple matrix texture to 2-d and 3-d porewater flow fields. In other words, a quantification of the permeability gradient at the scale of interest (i.e., a few millimeters) is required to constrain flow patterns and to augment predictive capability of biogeochemical transport and reaction models.

Most published profiles of hydraulic conductivity in natural soils derive from groundwater or oil reservoir research. For instance, Chappell et al. (1998) show the vertical decrease in hydraulic conductivity (from 50×10^{-6} ms^{-1} to an asymptotic K of 1×10^{-6} m s^{-1} at 1.5 m depth) on a 12 km^2 hillslope catchment area in Borneu, using a ring permeameter (Chappell and Ternan 1997). Field scale pump tests and laboratory core permeability tests were used by Olson et al. (2001) to show layered soil permeability to air on a scale of tens of centimeters in Picatinny Arsenal, NJ, USA. Multilevel slug testing in boreholes was used by Zlotnik and McGuire (1998) to report vertical K variability on a gravel and sand aquifer in Nebraska, USA, over a scale of tens of centimeters. Hydraulic conductivity depth profiles have also been measured in oceanic sediments at a scale of tens of meters and a resolution of about 2 m by Hart and Hammond (2002), using the Manheim squeezer. This method is designed to extract pore fluids from unconsolidated soil samples, by applying unidirectional pressure on an encased sediment sample and thus expelling porewater (Hart and Hammond 2002). However, hydraulic conductivity depth gradients with a resolution of a few millimeters have not been published before, to our knowledge.

In this paper, we propose a new method to obtain high-resolution permeability gradients in natural sandy sediments. If Darcy's law is applicable for the sediments and flow conditions under scrutiny, the proposed methodology allows a reconstruction of the vertical anisotropy in permeability for natural sediments, with a depth resolution of a few millimeters. This method, providing the necessary information on the possible range of advective flow crossing the water-sediment boundary layer in sandy sediments, was tested in natural North Sea sediments.

Materials and procedures

Falling head permeametry—Hydraulic conductivity (permeability) quantification relies on the measurement of flow rates through samples of soil, driven by a gravitational or other artificially induced hydraulic gradient. When it is clearly established that flow is at steady state (Klute and Dirksen 1986), Darcy's law (or its modification to local conditions, viz. ring permeameter, Chappell and Ternan 1997) is then applied to the results to extract *K*. Strictly in terms of methodological principle, two possibilities arise. Either a constant hydraulic gradient is applied to the sample, and volume of outflowing water is measured against time (constant head permeametry), or head is allowed to drop while water is flowing out through the sample, and the time gradient of the head is then used as data to extract permeability (falling head permeametry). Traditional methods to observe flow in this context suffer from a number of limitations. These include magnitude and rates that can be observed and the smoothness and quantity of the resulting data for each sample. For instance, electronic scales might be used to quantify the outflowing volume of water (Borcher et al. 1987). However, as amply discussed by Troyer and Skopp (1987), because scales are designed for quantifying a time average of a static mass, they are not ideally suited for the rapid, precise, and accurate measurements needed for samples with high permeability (sands and gravels).

Using pressure transducers to accurately measure head drop in falling head permeametry can obviate these limitations. In fact, they offer easy and precise calibration, the ability to measure pressure data in short time intervals (typically, less than 1/10 of a second), and simple interface and control with computer hardware, with precise control in timing, given by readily available freeware (e.g., Picolog and others). Last but not least, they are inexpensive compared to other measuring devices (electronic scales, electromagnetic flow meters, etc.). The quick response, precision, and small time-steps on data acquisition also allow measurement of rapid water flow through thin sections of highly permeable samples. This approach yields large and smooth datasets, suitable for modeling with Darcy's law with very small statistical error.

Micro-scale anisotropy in permeability—Natural sediments are not isotropic, even at a scale of a few millimeters. However, in marine deposits, the sediment bedding plane is often parallel to the sediment strata. The permeability, *K*, often approaches isotropy in the direction parallel to the bedding plane for each depositional stratum, but is generally anisotropic perpendicular to it. Small scale anisotropy in *K* can therefore be described as parallel or perpendicular to the direction of flow (Cardwell and Parsons 1945). If water movement through the sediment is to be predicted, this variation has to be understood.

Cardwell and Parsons (1945) used an electrical analogy (Ohm's Law) to establish the upper and lower bounds of composite permeability in a given direction. More recently, Le Loc'h (1987) used a variational method to confirm their results. For horizontal interstitial flow parallel to the bedding plane, the composite *K* is the arithmetic mean of the permeability of individual layers, and thus flow is dominated by the most permeable layers. However, for flow normal to the bedding plane, the composite *K* is the harmonic mean of the permeability of each superimposed layer, and thus smaller than the latter, because less permeable layers constrain flow in this direction (Tindall and Kunkel 1999). Obviously, this analysis is invalid if coherent vertical pathways of very high permeability (infauna burrows) intersect the sample. Even if we accept that in noncohesive sands this obstacle might still persist, it is still a fact that has to be dealt with in 2-d mapping of interstitial flow fields in any other circumstance, and one which is present for all other permeability determination methodologies. However, this subject falls outside the scope of this paper and is left as additional information for the reader.

An anisotropic, layered medium of this type can then be modeled as an anisotropic homogeneous medium in which K_L (the composite permeability for the whole sample of length *L*) depends on the resistance to flow through each of the superimposed sediment layers. Each layer "*i*" of thickness d_i has a different permeability, K_i. If just one layer composed the medium, the permeability *K* would be simply calculated by integrating Darcy's law in differential form. However, for a layered medium, the composite vertical *K* will depend on resistance to flow through each layer. By consequence, the hydraulic resistance, *R* (derived from Ohm's law), is such as $R = d_i/K_i$. Composite permeability for the whole system, K_L, would then be given by the quotient between the thickness of the sample (*L*) and the summation of resistances to flow imposed by all the individual layers with different hydraulic characteristics (Cardwell and Parsons 1945; Tindall and Kunkel 1999):

$$K_L = \frac{\sum_{i=1}^{L} d}{\sum_{i=1}^{L}\left(\frac{d_i}{K_i}\right)} \quad (1)$$

Stated simply, the problem (Fig. 1) is calculating the permeability of each superimposed layer of thickness d_i, knowing the composite permeability of two combined layers (K_L in Fig. 1) and of the layer of thickness $d_{i=2}$ (K_2), whereupon Eq. 1 can be applied to extract the *K* value for the target layer (K_1). If high-resolution measurements are available in a vertical sequence, this procedure can be successively applied to a whole core. Dubbed the Cardwell and Parsons bounds, this has been the established calculation procedure to quantify hydraulic conductivity depth gradients in a variety of porous media (e.g., Beckwith et al. 2003; Liu et al. 2002; Maulé et al. 2000).

We did this by determining the composite vertical permeability (K_L), then slicing off the topmost layer of thickness d_i, and subsequently determining the composite permeability of the leftover core ($K_{L\text{-}di}$), and so on. It is then a matter of apply-

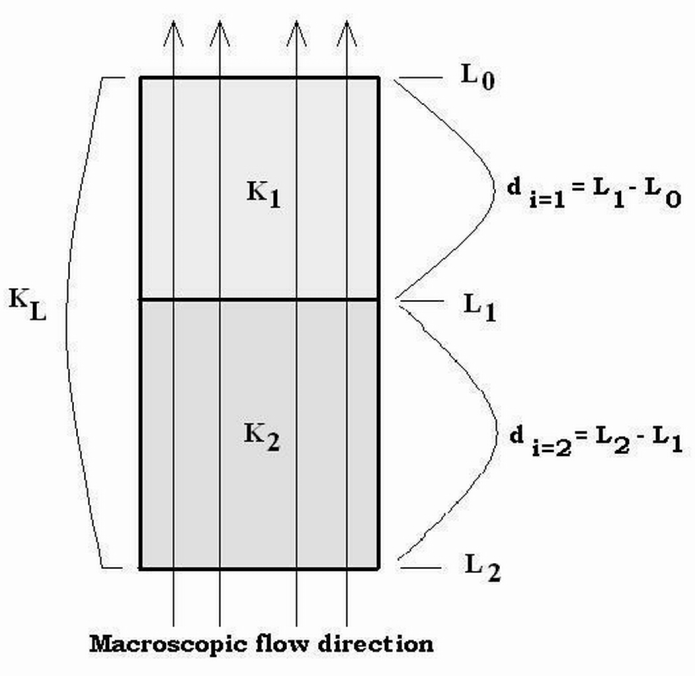

Fig. 1. Illustration showing the relationship between composite permeability and individual layer permeability in stratified sediment subject to flow normal to the sand layers. K_L is the composite permeability of the whole core, which results from the resistance to flow imposed by two layers with thicknesses $L_2 - L_1$ and $L_1 - L_0$, and individual permeability of K_2 and K_1, respectively (*see* Eq. 1 in text).

ing Eq. 1 in reverse succession to determine the contribution by each superimposed layer to the overall composite permeability. The operational limit of this "decomposition" procedure is set at the upper end of analytical error associated with the measurement of permeability by falling-head permeametry, for each layer. Because the error associated with each measurement will accumulate (Miller and Miller 1984) with that associated with the other measurements during "decomposition," the methodology used to measure hydraulic conductivity should have a very high precision.

Procedures—The relationship between hydraulic conductivity, k (cm s^{-1}), and loss of head through time in a falling head permeameter follows directly from the principle of mass conservation and Darcy's law (Domenico and Schwartz 1991) and is as follows:

$$k = \left(\frac{aL}{At}\right) ln\left(\frac{h_0}{h_f}\right) \quad (2)$$

where a is the sectional area of the stand-pipe (cm^2), A the cross-sectional area of the sediment sample (cm^2), L the length of the sample in the macroscopic flow direction (cm), t the elapsed time since the beginning of the test (s), h_0 the height of water in the stand pipe above discharge level at time t_0 (cm), and h_f the height of water in the stand pipe above discharge level at time t (cm). Hydraulic conductivity was determined on board, using falling head permeametry with two different experimental setups per sample. In each test, filtered (0.2 µm) seawater from the same sampling station was used. This was done to ensure that water permeating through the sample had salinity as close as possible to the local porewater, and that no fine particulates present would eventually decrease the test-sample's hydraulic conductivity by clogging of the natural pore structure with finer particles and organic colloids (Barrington et al. 1987; Rowsell et al. 1985). To avoid flow instability and air entrapment effects on flow rate (Wang et al. 1998), cores were kept water saturated during tests (overlying water column in excess of 1 cm length). In addition, while waiting for experimental procedures, cores were sealed to preclude any evaporation and subsequent artifacts due to increased salinity (flow fingering, Wang et al. 1998).

With one setup, k was determined at intervals of roughly 0 to 10 cm, 0 to 6 cm, and 0 to 3 cm sediment depth on 3.6 cm diameter cores. Intervals deviated depending on the actual slicing position. Cores were placed onto a sand-bed with a porous screen preventing the core from spilling. The sandbed had a k value in large excess of the sample core. Times for six consecutive steps of falling head (1 cm) were noted for each core length (L), and k was calculated according to a simplified version of Eq. 2, viz:

$$k = L\frac{ln\left(h_1/h_2\right)}{\Delta t} \quad (3)$$

with h_1 and h_2 being the hydraulic head before and after the measurement, respectively, and Δt being the time elapsed between measurements. From these, a standard error for each measurement was determined ($n = 6$).

With the other setup (Fig. 2), head drop was recorded through time at intervals of roughly 0 to 5 cm, 0.3 to 5 cm, 0.6 to 5 cm, 0.8 to 5 cm, 1.0 to 5 cm, 1.3 to 5 cm, 1.5 to 5 cm, 1.8 to 5 cm, 2.0 to 5 cm, 2.3 to 5 cm, 2.5 to 5 cm, 2.8 to 5 cm, and 3.0 to 5 cm on 2-cm diameter sediment cores. Depth intervals deviated depending on the actual slicing position. Height of water above discharge level was measured by a sensitive pressure transducer (blood pressure transducer, World Precision Instruments), generally at 1-second intervals, depending on the actual permeability of the core and the expected duration of the run. A minimum of 100 measurements was taken for every measuring run. The k value was calculated by linear regression analysis at the 99% confidence interval of the plot of $Ln\ (h_0/h_f)$ as a function of time according to Eq. 2. The compliance of data to Darcy's law was verified from the linearity of the plot, since it is only valid for steady state flow (Klute and Dirksen 1986; Klute 1965). During the first tens of seconds of each experimental run, adaptation to steady state flow showed as a deviation from linearity of the plot of $Ln\ (h_0/h_f)$ as a function of time. This data were discarded prior to regression analysis. All hydraulic conductivity (k, cm s^{-1}) data were converted to permeability (K, m^2) normalized to 20°C and 34.5 PSU (as in Klute 1965) using $K = k\mu/g\rho$, where µ is dynamic viscosity (1.0827×10^{-2} g

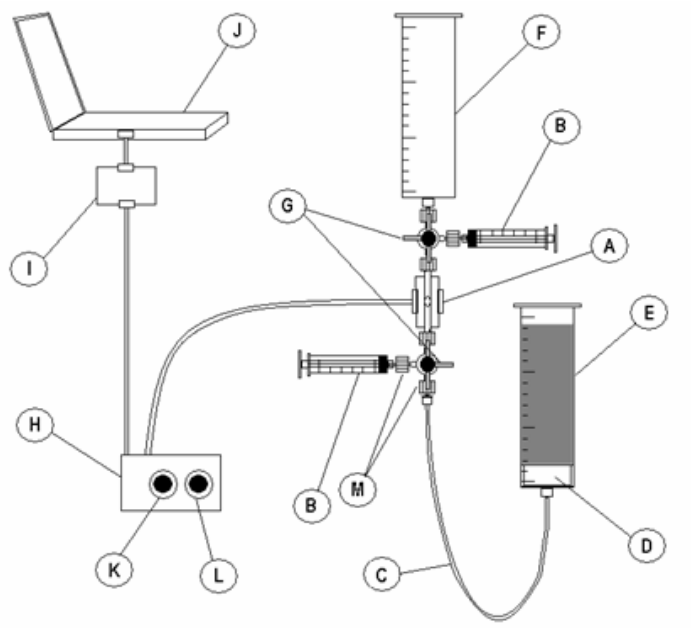

Fig. 2. Experimental setup developed for precise falling head permeametry in marine sediment samples identified in text as Setup 2. (a) Blood pressure transducer, (b) transducer debubbling syringes, (c) Tygon tubing, same diameter as transducer flow path, (d) porous screen, allowing maintenance of sample integrity, (e) sediment core, inside syringe, (f) water standpipe, (g) three-way stopcocks, allowing easy start/stop of flow and debubbling of transducer flowpath, (h) voltage conditioner/signal amplifier, (i) 16-bit DAC (Pico Technologies ADC-16 Datalogger), (j) laptop with Picolog data acquisition software, (k) excitation voltage dial (1-10 VDC), (l) signal amplification dial, and (m) Luer locks.

$cm^{-1}\ s^{-1}$), g is gravitational acceleration (9.81×10^2 cm s^{-2}), and ρ is water density (1.01 g cm^{-3}). No relevant temperature and density gradients were expected in the first few centimeters of sediment, because the chosen sampling site has a seawater column in excess of 20 m. Use of this methodology in coastal intertidal sediments or other sites where depth-related gradients in density and temperature of the porewaters are expected (Rocha 1998, 2000; Webster et al. 1996) has to take them into account. All measurements can be normalized to the same temperature and density while converting hydraulic conductivity to permeability (as in Klute 1965), for comparison sake, but transient porewater flow modeling has to ensure that changes of permeability with time occur in response to changing temperature and density gradients.

Core sectioning—A potential problem with the use of permeameters is the leakage between the soil sample and the permeameter wall (Baker and Bouma 1975). The possibility of a flow short-circuit around the test sample is inversely proportional to the hydraulic conductivity of the sample. For example, methodologies for testing low permeability samples (e.g., peat, clays) need great care to ensure that no cross-circuiting of flow takes place: clay (Baker and Bouma 1975) and peat (Beckwith et al. 2003) samples are encased in gypsum prior to testing. In the case of highly permeable samples such as the ones used in this work (unconsolidated sands), this could be effectively disregarded, because the available space between the sediments and the core liners is of the same order of magnitude or less than the connected pore space through the sample. However, the problem of sectioning the sample cores during testing arises. Two alternatives were considered: either the core was pushed out of the liner, sectioned, and pulled in again (suction) using the syringe plunger, or the core was sectioned by carefully scraping off the surface of the sediment with a fine-edged spatula until the desired core length for the second test was reached. Attempts with the first method proved to disturb the sample to an unacceptable extent: desegregation, air bubble intrusion between the sample and the liner prior to retesting, and decompaction of the sample all took place to various degrees, proving that this would not be the most correct method for shortening the sample under test. This method was thus abandoned. We opted for the second method, in which the water column on the core was carefully removed using tissue paper after the first length was tested, until only a couple of millimeters of water were left. A fine spatula was then introduced into the core and a thin layer carefully scraped off. The core was resaturated from below before retesting.

Typically, this sectioning procedure was referenced to the outer volume markings on the syringe, so that compaction could be controlled when putting in the upper porous seal. Use of this method precludes fine control over which depths are going to be tested. However, it disallows changes to sample compaction, desaturation, and air bubble intrusion, the greatest sources of error in permeametry (Wang et al. 1998; Klute and Dirksen 1986; Klute 1965).

Assessment

Sampling site—Sandy sediment cores were taken from five stations (Station A at 51°53′N, 3°47′E, to Station E at 53°05′N, 3°46′E) on the Broadfourteens in the North Sea and analyzed by both setups. Water content varied from 17.3% at station B and 19.6% at station C. Superficial median grain size (d_{50}) of the uppermost sediment ranged from 243 µm at station A to 232 µm at station E. On deck, cores were sub-sampled from box-cores with acrylic liners (setup 1) and cut-off syringes (setup 2), and immediately carried to the lab for analysis.

Coring—Sediment cores were obtained using a cylindrical boxcorer, developed at the Royal Netherlands Institute for Sea Research (NIOZ). The boxcorer was equipped with a hydraulically dampened closing lid to avoid pressure artifacts during core retrieval. The bottom of the boxcorer was sealed with a rubber plate during retrieval to prevent percolation of water through the sediment column. Prior to subsampling, retrieved box cores were evaluated on deck for percolation and for possible damage to the sediment's surficial layer. Overlying water (>15 cm depth) was inspected for traces of turbidity, sign of resuspension of the surface sedi-

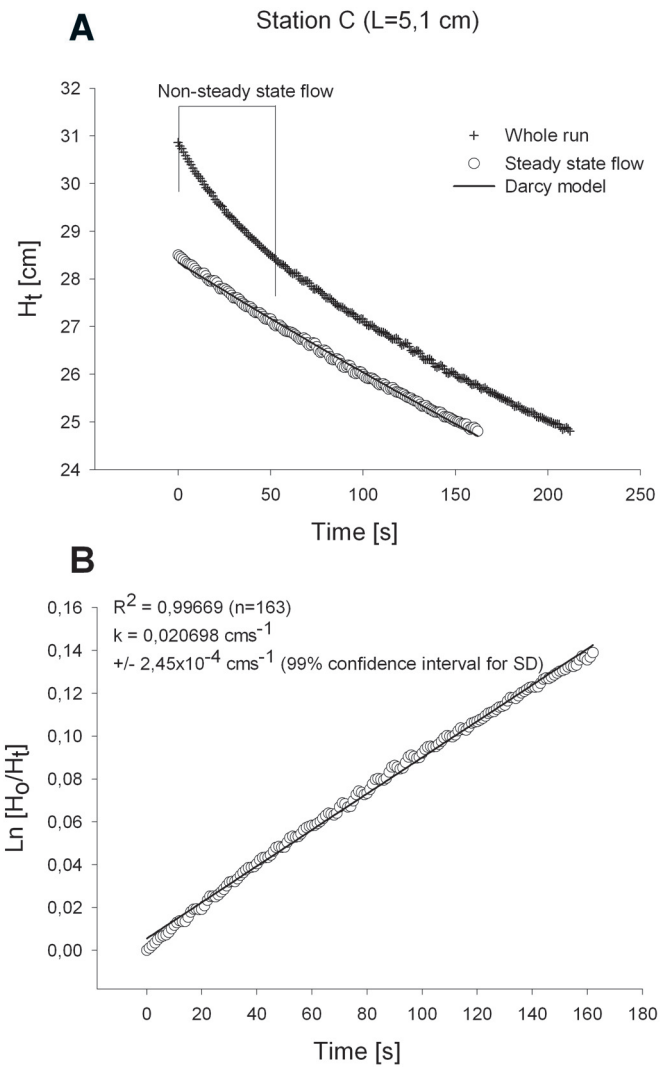

Fig. 3. Illustrative plot of full measurement run and preliminary data treatment for extracting permeability for station C, length of core (L) of 5.1 cm. (A) Curve on top: Change in hydraulic head with time, for the whole run. Note non–steady state flow during first 50 s, data that will be rejected before extracting the permeability; lower curve: re-plot of the part of data complying with steady-state flow, with superimposed values of Darcy's model. (B) Plot of linear version of Darcy's law and linear regression analysis on retained data (see A), giving the estimated composite permeability (k) and associated error.

ment layer. When turbidity was observed, the collected sediment core was discarded and the box corer redeployed. Leakage of the core was verified by cleaning the outer surface of the liner with a handcloth and then checking for water trickling through the bottom rubber seal. When this happened, the sediment was discarded and the corer redeployed. When sub-sampling the box-core sediment, compaction of the sub-sampled core was assessed after the core liner was driven into the sediment, by measuring the difference between the level of the sediment surface inside the core liner and its level outside the pipe. No compression greater than 1 mm (typically <2% core length) was observed. To avoid possible suction artifacts while retrieving sub-samples, a rubber stopcock was pushed into the bottom of the buried core liner through the adjacent sand. This was done after all the necessary sub-sample core liners for a given box-core were already driven into the sediment.

Permeametry—Falling head as computed by Darcy's law was fitted to the measured data of head and time using the Solver routine of Microsoft Excel according to

$$h = h_0 e^{-(kt/L)} \tag{4}$$

As expected, the first tens of seconds of each measurement run did not comply with the steady state conditions assumed by Darcy's law, whereupon these data were excluded from further analysis (Fig. 3A). This trend was particularly visible when using setup 2, due to the high sampling frequency and large number of readings. The value for hydraulic conductivity and associated estimate error was extracted from the plot of head against time, by regression analysis using the linear version of Darcy's law (Fig. 3B). Hydraulic conductivity for successive measurements on the same core (station E) with both setups is shown in Fig. 4 for illustration purposes. Complete results for the five stations using setup 2 are condensed in Table 1. Because it showed much higher precision relative to setup 1 (Fig. 4), only results obtained by setup 2 were used to calculate permeability gradients for the depth scale of the oxic layer.

Calculations—Once composite permeability values are available by process of sequential measurements on diminishing core plugs, individual layer permeability can be extracted using Eq. 1. However, this process is not sufficient. The initial estimate of individual layer permeability is derived by direct application of Eq. 1 in sequential fashion to each dataset. Each *k* value is successively extracted from pairs of composite permeability values, starting from the bottom of the core: as in Fig. 1 and so on upward until complete treatment of the whole core is accomplished. However, this procedure does not account for individual uncertainty (Table 1). Due to the law of propagation of errors, individual errors for each pair of permeability values will accumulate every time Eq. 1 is applied during profile decomposition. This way, a realistic profile showing individual *k* values is often not directly obtainable. Negative values of individual layer *k* sometimes arise from the calculation, during the last stages of decomposition (e.g., the topmost few millimeters). The process is then refined from this initial "guess" by resorting to nonlinear curve fitting, using the Levenberg-Marquardt method (Press et al. 1986). From starting values of individual parameters (in the present case, the first calculation for individual layer permeability), this algorithm seeks to minimize

Table 1. Composite permeability (K m^2) values obtained in successively diminishing core plugs for all stations by setup 2

Station and length (cm)	*n**	*K* (m^2)	SD† (%)
A			
4.0	202	7.268×10^{-12}	2.49
3.8	152	1.412×10^{-11}	2.02
3.5	410	1.145×10^{-11}	0.54
3.3	211	1.236×10^{-11}	1.76
3.0	332	1.148×10^{-11}	0.53
2.7	230	1.288×10^{-11}	1.21
2.5	240	3.048×10^{-11}	0.33
2.3	280	1.387×10^{-11}	0.76
2.1	217	9.652×10^{-12}	0.75
B			
4.2	188	1.305×10^{-11}	1.42
3.9	257	1.302×10^{-11}	0.96
3.7	234	1.174×10^{-11}	1.46
3.1	224	1.497×10^{-11}	4.26
2.9	225	1.444×10^{-11}	1.01
2.7	212	1.339×10^{-11}	0.63
2.5	153	1.339×10^{-11}	0.63
2.3	215	1.032×10^{-11}	1.09
C			
5.1	163	2.089×10^{-11}	1.18
4.8	164	1.686×10^{-11}	1.15
4.4	165	1.655×10^{-11}	0.90
3.2	233	1.025×10^{-11}	0.96
3.0	213	1.233×10^{-11}	0.79
D			
4.7	321	1.370×10^{-11}	0.58
4.5	485	1.152×10^{-11}	0.44
4.1	291	1.168×10^{-11}	1.25
3.8	407	1.049×10^{-11}	0.38
3.6	362	1.231×10^{-11}	0.39
3.2	424	1.092×10^{-11}	0.34
3.0	425	4.232×10^{-12}	0.92
2.8	306	5.505×10^{-12}	0.92
2.5	435	6.554×10^{-12}	0.62
2.3	392	6.161×10^{-12}	0.42
E			
5.0	440	1.518×10^{-11}	0.53
4.7	435	1.351×10^{-11}	0.47
4.4	353	1.266×10^{-11}	0.51
4.1	435	1.211×10^{-11}	0.59
3.8	339	1.369×10^{-11}	1.63
3.5	218	1.252×10^{-11}	1.02
3.3	243	1.200×10^{-11}	0.76
3.0	181	1.168×10^{-11}	1.06
2.8	184	1.232×10^{-11}	0.94
2.6	262	1.089×10^{-11}	0.89
2.3	214	4.969×10^{-12}	2.43

*Number of data points for each determination is identified by *n*.
†Respective standard deviation in percentage at the 99% confidence level.

$$\chi^2(K_L, K_2) = \sum_{i=1}^{N} \left[\frac{K_L^{measured} - K_L^{estimated}}{\sigma_i} \right]^2 \quad (5)$$

where $K_L^{measured}$ is the measured composite permeability for a sediment plug with height equal to L, K_2 is the measured composite permeability for $d_i = 2 = L_2 - L_1$ (see Fig. 1 for support), $K_L^{estimated}$ is composite permeability calculated for the same L using Eq. 1, based on individual layer permeability contributions, and $/\sigma/_i$ is the standard deviation associated with the k estimate from falling head measurements for $K_L^{measured}$. With the convergence criterion used by the Levenberg-Marquardt method, higher tolerance is applied for iteration procedures on variables that have a greater known uncertainty (Press et al. 1986).

"Overshooting" or walk-away values for individual parameters (in our case, individual layer permeability values) can sometimes occur while iterating to minimize $/\chi/^2$. These arise when $/\chi/^2$ keeps decreasing during iteration, while individual k estimates surpass physically realistic values. An individual sensitivity analysis is then performed for each k value, where its change is compared with the concomitant variation in $/\chi/^2$ for a large range of k values. A practical value for k is then picked by selecting the last iterative solution for k that lowers the convergence criterion by the smallest admissible error associated with the measurement procedure (in our case, $/\sigma/_i$ at 99% confidence interval). A comparison between $K_L^{measured}$ and $K_L^{estimated}$ obtained this way during the decomposition procedure is shown in Fig. 5 for all five stations. All calculations followed standard methods of error propagation (Miller and Miller 1984). Consequently, errors attributed to each recalculated composite k value can be observed to increase toward the surface of the core in the recomposition procedure (Fig. 5). Resultant high-resolution permeability gradients are shown in Fig. 6A.

Reproducibility and intercomparison of methods—Consecutive tests over a single core might have introduced an error on the measurement of successive hydraulic conductivities. As mentioned before, artifacts due to clogging by fine particulates and organic colloids were effectively eliminated by using fine-filtered seawater (0.2 µm). Still, repeated trickling of water through the same core layer might wash out fine particles resting inside larger pores, or change its degree of compaction. To assess reproducibility of the k measurements, repeated (14 consecutive test runs) were carried out on sandy sediment cores with 4 different lengths (6.8, 6.3, 5, and 4 cm) taken at an intertidal site in the Ria Formosa lagoon, South Portugal. Median grain size (d_{50}) ranged from 250 µm (test III, L = 4 cm) to 355 µm (test II, L = 6.3 cm). Resultant hydraulic conductivities are shown in Fig. 7. If some error-inducing artifact of the measurement procedure would cause a second reading over the same core to be higher or lower than the first, this artifact would also cause the third to be higher/lower than the second and so on. It is clear from the plot that no such behavior was apparent, suggesting that the method is reproducible, at least for sands. In addition, Kolmogorov-Smirnov normality tests

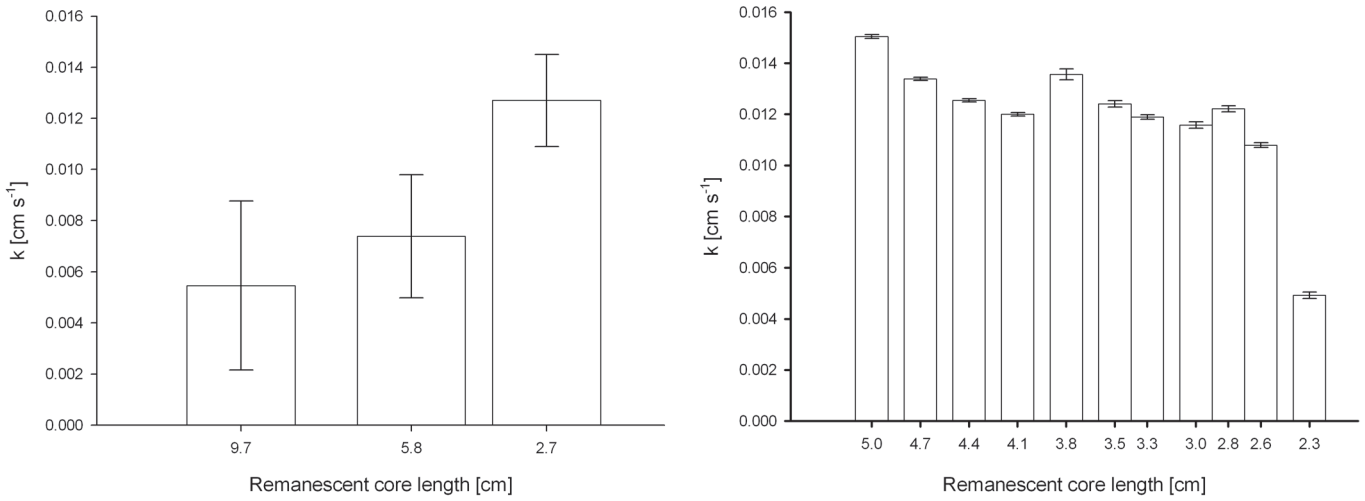

Fig. 4. Comparison between permeability measurements by both setups in samples from station E. The first bar in each plot represents *k* for the whole core. Subsequent bars to the right represent k of the reminiscent length after consecutive layers where removed. The left hand side graph corresponds to procedure 1 (slicing upwards from the bottom of the core), showing permeability determined in three sub-cores of the original 9.7 cm long sample. Right hand side corresponds to procedure 2 (slicing from the top of the core downwards), showing permeability determined by successive shortening of a 5-cm long core into 11 consecutively smaller sub-cores. Error bars represent SD of permeability estimate at the 99% confidence level.

(SPSS Inc. Sigmastat version 2.03) were applied to each data set to test whether such a succession of values would arise from a normal distributed population. Deviation from normality of the results would be evidence of a systematic error in methodology (Miller and Miller 1984). All measurement runs passed the Kolmogorov-Smirnov normality tests (Test I, $K - S_{dist} = 0.200$, $P = 0.134$, $n = 14$; Test II, $K - S_{dist} = 0.200$, $P > 0.200$, $n = 14$; Test III, $K - S_{dist} = 0.190$, $P = 0.185$, $n = 14$; Test IV, $K\text{-}S_{dist} = 0.185$, $P > 0.200$, $n = 14$). Also, the low variability about the mean (standard deviation, as a percentage of average k, $n = 14$, ranged from 0.2% on Test I to 1.2% on Test II) was similar to errors associated with shipboard measurements (Table 1). Thus, the reproducibility analysis shows that repeated testing of the same sample by our method did not cause systematic changes to *k*, suggesting that our values of hydraulic conductivity are reliable and not a function of time.

As an additional check of the validity of the method, results from both procedures were compared for analogous sediment samples. This was accomplished by reconstructing (Eq. 1) the composite permeability for the exact same core length, using the individual layer *k*'s (Fig. 6 A) determined by procedure 2, and comparing the result with the measurements in the topmost 2- to 3-cm plug obtained by procedure 1. The comparison is shown on Fig. 8. The similarity is evident, because both setups predict almost the same composite permeability for the same 2 to 3 cm sediment surface layer at each station. In conjunction with high reproducibility (Fig. 7), this result, added to the striking correspondence between successive composite measurements of *k* in the same core and their respective reconstruction using the individual layer *k*'s for all stations (Fig. 5), consolidates the validity of the whole methodology.

Applying Cardwell and Parsons (1945) bounds to determine 2-d permeability—As stated before, marine deposits usually have the bedding plane parallel to the sand strata. It follows that if the two coordinates are set in the bedding plane (x parallel to the sand strata and z normal to the sand-water interface), the two vector components for horizontal (k_h) and vertical (k_v) permeability can be derived, thus defining the anisotropy of the medium. This methodology is used with success in computer algorithms to quantify equivalent hydraulic conductivity of heterogeneous media (*see* Renard et al. 2000 and references therein). Calculations are straightforward, keeping in mind that the pressure gradient driving the flow into the porous medium is established at the sand-water interface either by drag, wave oscillation, or ripple intersection of the flow. Thus, the described method and its results allow us to calculate the two normal components of the 2-d permeability tensor. The law of harmonic averages (Eq. 1) is used to calculate the resultant vertical tensor component (k_v) at a certain depth below the interface, and the arithmetic mean of *k* values of contributing strata to calculate the horizontal component (k_h) at that depth. The anisotropy of the medium, defined by the ratio k_v / k_h, is also an important dimension in the quantification of flow through a porous medium, because it allows geometrical scaling of the normal components of the 2-d permeability tensor. This technique leads to greater simplification of the governing flow equations on these media (Phillips 1991). Anisotropy of the five samples collected at the North Sea is plotted in Fig. 6B. Note that because of the underlying assumptions of the decomposition procedure (*see* Materials and procedures), the topmost layer always appears as

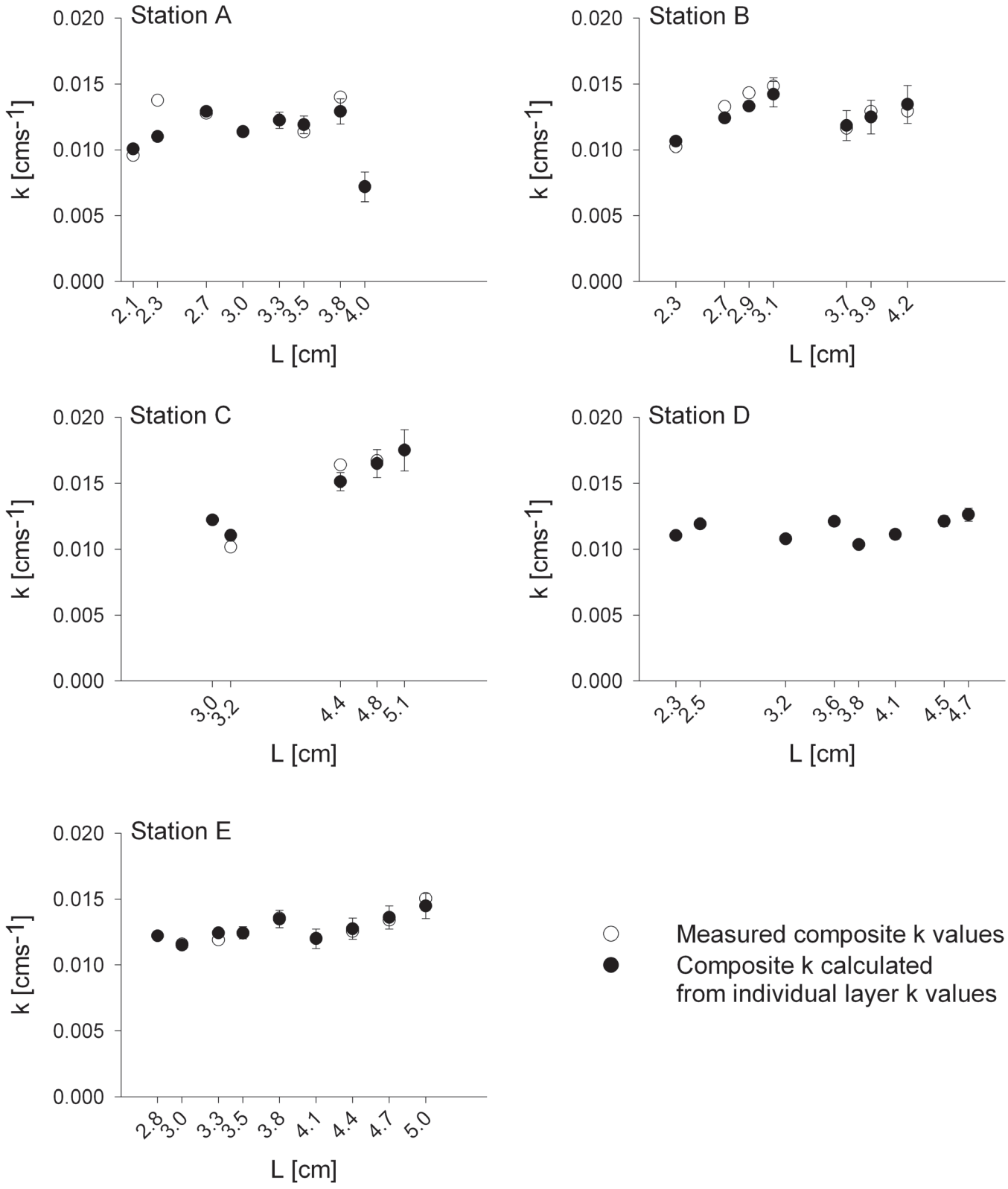

Fig. 5. Comparison between the permeability determined for each sample in successively diminishing core plugs ($K_L^{measured}$) and the reconstructed permeability emulating $K_L^{measured}$ by using individual layer k values obtained by decomposition procedure ($K_L^{estimated}$) for all five stations. For further explanation, *see* text.

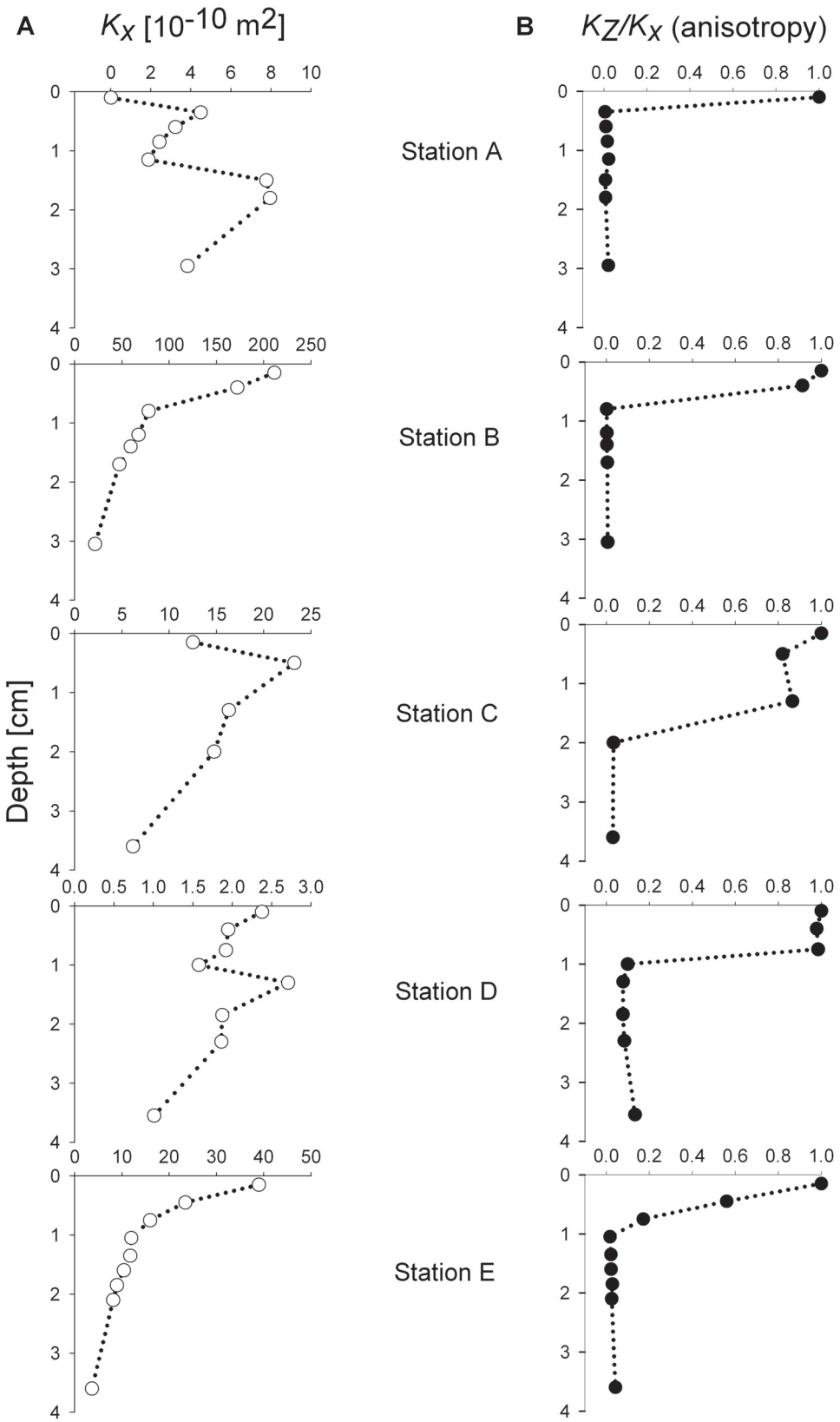

Fig. 6. Plots showing high resolution permeability depth profiles obtained for all five sampled stations (A) and concomitant anisotropy gradients (B).

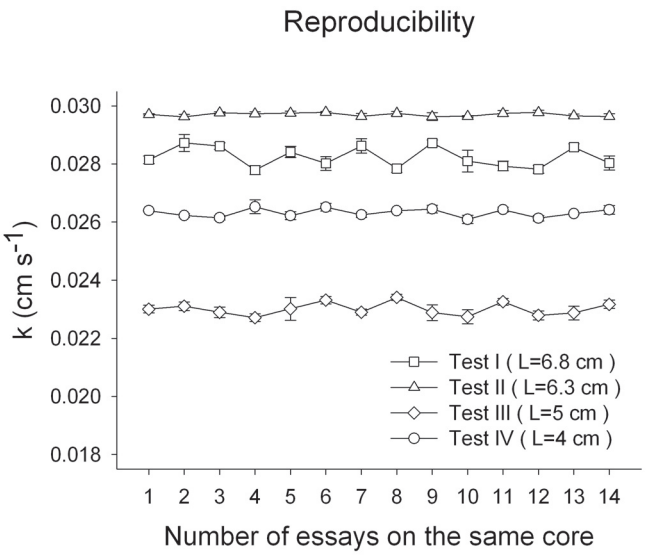

Fig. 7. Graph showing reproducibility of permeability obtained with setup 2 in successive tests on the same sample. Tests were carried out with sand core samples with different lengths taken in intertidal sandy sediment of the Ria Formosa lagoon, South Portugal. Median grain size (D_{50}) of samples ranged from 0.250 µm (Test III) to 0.355 µm (Test II). Average K (cm s^{-1}) ± SD per core test: Test I (L = 6.8 cm, n = 14), 0.0282 ± 3.57 × 10^{-4}; Test II (L = 6.3 cm, n = 14), 0.0297 ± 5.9 × 10^{-5}; Test III (L = 5 cm, n = 14), 0.0230 ± 2.18 × 10^{-4}; Test IV (L = 4 cm, n = 14), 0.0263 ± 1.45 × 10^{-4}.

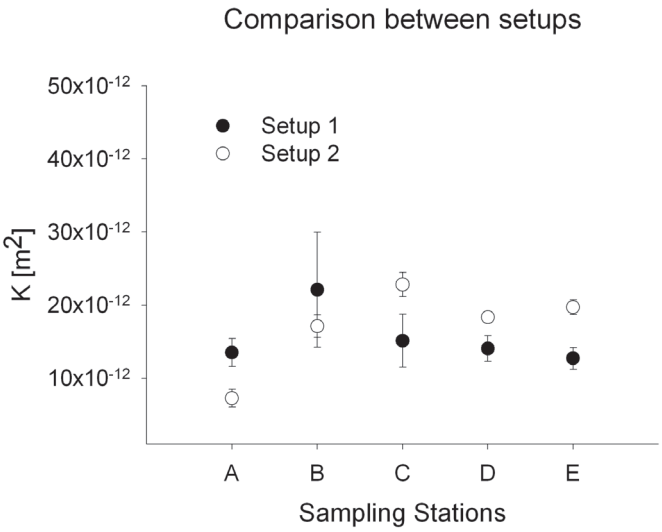

Fig. 8. Graph comparing the composite permeability obtained by both procedures on sediment plugs of equal length for all sampled stations. Error bars represent standard deviation at the 99% confidence interval.

isotropic. That is, the ratio k_v / k_h is equal to 1, meaning that the permeability tensor is diagonal, making an angle into the sediment of arctangent of k_v / k_h, 45º in this case.

Interpretation of high-resolution K gradients—Micro-anisotropy of natural sandy sediments is revealed by the high resolution permeability gradients obtained for the five stations in the North Sea (Fig. 6A). Using the Carman-Kozeny approach to estimate the permeability of the top surface layers from mean grain size and porosity (Boudreau 1997), gives values ranging from a minimum of 3.45 × 10^{-11} m^2 at station B to a maximum of 5.31 × 10^{-11} m^2 at station C. Indeed, both procedures used on board yield composite permeability within the same order of magnitude (Fig. 8) for the top 2 to 3 cm sediment plug. The less precise procedure measures higher permeability at station B (2.21 ± 0.785 × 10^{-11} m^2) compared to A, C, D, and E, whereas procedure 2 gauges higher permeability for station C (2.28 ± 0.167 × 10^{-11} m^2), which is in better accordance with the Carman-Kozeny estimate for the range in all stations. Despite the close agreement between the two methods, sediments in reality often show great disparity in geometrical scaling along and across the bed; relatively low permeability layers intercalate with much more permeable ones, so that the variations in the vertical direction are much more rapid than those along the horizontal (Phillips 1991). This is clearly demonstrated in the high resolution gradients (Fig. 6A): whereas on stations B and E permeability decreased rapidly with depth, for the other stations more permeable layers were sandwiched between less permeable ones. The question of geometrical scaling of these changes, in particular within the context of sediment-water fluxes, gains importance if we notice that the surficial couple of millimeters of station B reveal a permeability of 2.11 × 10^{-8} m^2, three orders of magnitude higher than composite values for the whole core (Table 1). If taken as representative of the whole core, this k value would correspond to a Brinkman layer of 0.145 mm, using the $\sqrt{K}$ criterion (Boudreau 1997) and between 2.9 and 14.5 mm, if based on laboratory evidence of the real extension of the Brinkman layer (Gupte and Advani 1997).

Discussion

The assessment results underline the need for high-resolution permeametry in order to correctly ascertain the range of advective interfacial flows in sandy sediments, as discussed in the introductory remarks. Insight into the vertical structure of the surface sediment layers and by consequence, into sedimentation-resuspension cycling in this area of the North Sea is also patent from the profiles. Sedimentation of very fine post-bloom material on the surface of sandy sediment would cause the surficial layer permeability to drop considerably compared to what happens beneath this horizon (Fig. 6A, Station A). Clogging of the sediment to some extent will occur simultaneously in regard to advective flow crossing the interface (notice overall permeability of station A is lower than that of the other stations, Fig. 8). Small ripple migration and resuspension events, by diminishing to different degrees the cohesiveness of the surface benthic layer, would produce

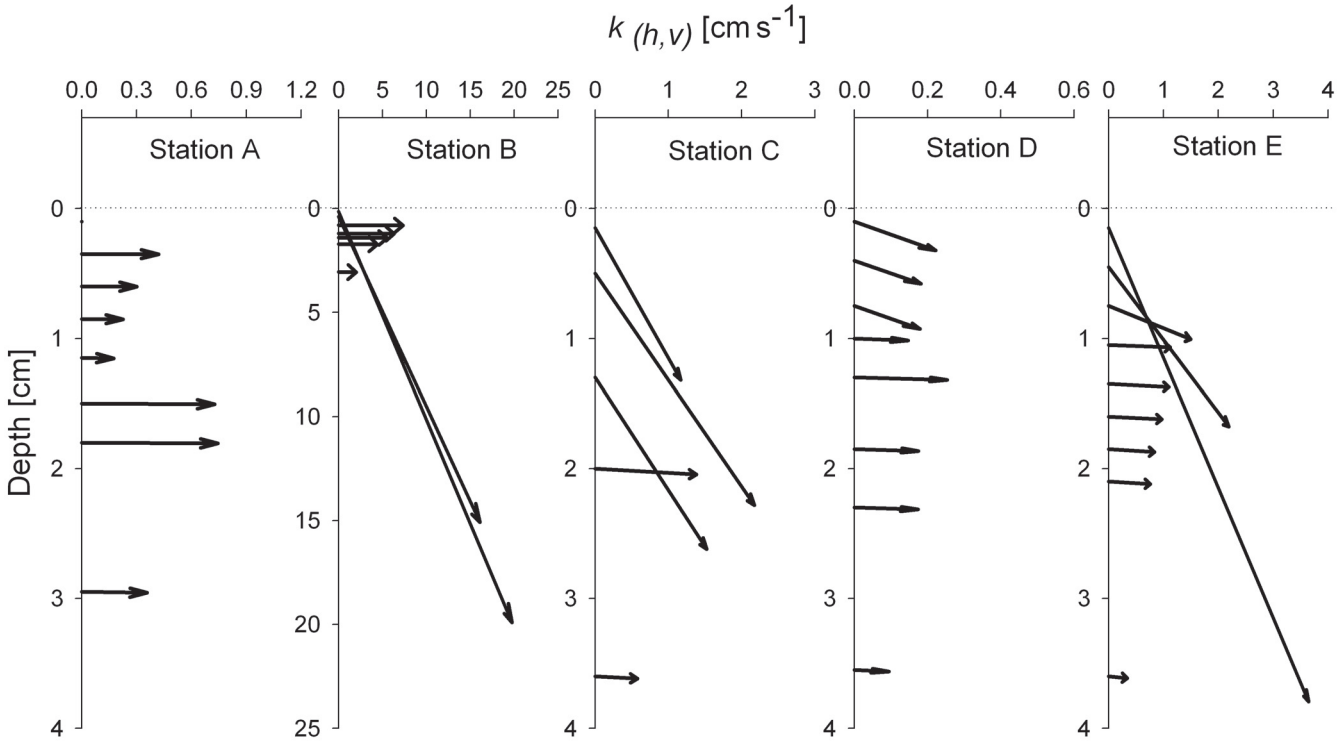

Fig. 9. Vector plots showing the change in direction and magnitude of the second-order permeability tensor, $k_{(h,v)}$, with depth for the five sampled stations.

abrupt shifts in the permeability gradients at the topmost 2 to 3 cm, compared to the deeper, more cohesive and compact sediment (Stations A, C, D, and E).

Additional insight into the viability to any extent of advective flow crossing the sediment water interface is provided by analysis of the anisotropy gradients for all stations (Fig. 6B). As stated previously, if the two coordinate directions within the bedding plane are perpendicular to each other, the ratio between vertical and horizontal component magnitudes of permeability (k_v/k_h) will permit calculation of the angle between the 2-d permeability tensor and the interface. For a k_v/k_h ratio of 1, this will be 45°. Notice that for stations B through D, the k_v/k_h ratio varied between 1 and 0.8, from the surface to 0.5-cm depth (station B), and even up to 1 cm depth and beyond (Stations C and D).

However, preferential flow pathways determined as described can best be visualized for all stations using vector plots (Fig. 9). At station A, very low permeability of the surficial layer (1.15×10^{-12} m^2, k_h and k_v are too small to appear in plot) conditioned the vertical component of k throughout the core, making it impermeable to penetrating flow. Even then, quite high horizontal permeability of underlying layers added up to a composite permeability of 7.268×10^{-12} m^2 for the whole core (Table 1). This is the perfect example of the utility and the step forward provided by this methodology: in theory, the composite permeability of the whole core would provide grounds for the existence of advective porewater exchange through the sediment-water interface (Huettel and Gust 1992). However, the results demonstrated the exact opposite: in reality, the very low permeability of the topmost 2 mm sediment effectively clogs the interface, making this particular stretch of bottom sediment impervious to advection through the interface. The opposite is shown by results of station B (Fig. 9, Station B): the top 0.5 cm layer was very permeable (Fig. 6A), the anisotropy was between 0.9 and 1, and consequently the permeability vector had a very high magnitude ($2.985 - 2.327 \times 10^{-8}$ m^2), and an angle of attack into the sediment between 40° and 45°. However, right below the 0.5-cm depth, vertical permeability (k_v) vanishes, meaning that the flow pathway would turn sharply upwards at this depth. The range of penetration of advective exchange in this stretch of sea bottom would be close to 0.5 cm. A "textbook example" is demonstrated by results from station E. Here, the vertical permeability component decreased slowly with depth in the sediment, concomitant with a decrease in magnitude of the 2-d permeability tensor; as a result, it is easily shown that the flow pathway will curve elegantly upwards from an angle of attack of 45° at the surface, passing through the horizontal at 1 cm depth. Both the advective flux, u, and the potential gradient,$\nabla\Phi$, proportional to the permeability second order tensor, $k_{(h,v)}$ (Phillips 1991; Dullien 1992), would justify an advective mixing layer 1 cm deep. In addition, the magnitude of the 2-d permeability tensor decreased from 5.51×10^{-9} m^2 at the surface to 1.2×10^{-9} m^2 at 1-cm depth. These values are

still three orders of magnitude higher than the composite permeability of 10^{-12} m^2 determined before as a cut-off for advective flow into sediments (Huettel and Gust 1992), and two orders of magnitude higher than the composite permeability of the whole core (Fig. 8, Table 1).

It has thus been demonstrated, with real samples, that with this methodology, both the direction and magnitude of the second order permeability tensor can be calculated from direct measurements. This result is a major improvement over previous methods in the particular context of studying flow and reaction in permeable sediments and answers the call put forth in Boudreau et al. (2001) and by SCOR WG 114. While providing a simple, measurable, and elegant explanation for the apparent misconception around the empirical barrier of 10^{-12} m^2 (Huettel and Gust 1992), these measurements forward a simple explanation to existing paradoxes, namely the higher-than-predicted depth reached by advection shown in previous studies (Güss 1998; Huettel et al. 1998; Huettel et al. 1996; Lohse et al. 1996; Booij et al. 1991). To our knowledge, it is the first time that the 2-d permeability tensor is determined for real sediment samples in the context of advective exchange through the sediment water boundary layer, a definite step forward in the comprehension of matrix parameters that condition water flow into the permeable sandy sea bottom.

References

Baker, F. G., and J. Bouma. 1975. Variability of hydraulic conductivity in two subsurface horizons of two silt loam soils. Soil Science Society of America J. 41:1029-1032.

Barrington, S. F., P. J. Jutras, and R. S. Broughton. 1987. The sealing of soils by manure. Part II. Sealing mechanisms. Can. Agric. Eng. 29(2):105-109.

Beckwith, C. W., A. J. Baird, and A. L. Heathwaite. 2003. Anisotropy and depth-related heterogeneity of hydraulic conductivity in a bog peat. I: Laboratory measurements. Hydrol. Process. 17:89-101.

Booij, K., W. Helder, and B. Sundby. 1991. Rapid redistribution of oxygen in a sandy sediment induced by changes in the flow velocity of the overlying water. Neth. J. Sea Res. 28(3):149-165.

Borcher, C. A., J. Skopp, D. Watts, and J. Schepers. 1987. Unsaturated hydraulic conductivity determination for fine-textured soils. Trans. ASAE 30:1038-1042.

Boudreau, B. P. 1997. Diagenetic models and their implementation. Modeling transport and reactions in aquatic sediments. Springer, Berlin.

——— and others. 2001. Permeable marine sediments: overturning an old paradigm. EOS82 (11):133-136.

Brinkman, H. C. 1947. On the permeability of media consisting of closely packed porous particles. Appl. Sci. Res. A1: 81-86.

Cardwell, W. T., and R. L. Parsons. 1945. Average permeabilities of heterogeneous oil sands. Trans. Am. Inst. Mining Met. Pet Eng. 160:34-42.

Chappell, N. A., S. W. Franks, and J. Larenus. 1998. Multi-scale permeability estimation for a tropical catchment. Hydrol. Process. 12:1507-1523.

Chappell, N. A., and L. Ternan. 1997. Ring permeametry: design, operation and error analysis. Earth Surf. Process. Landf. 22:1197-1205.

Dagan, G. 1984. Solute transport in heterogeneous porous formations. J. Fluid Mech. 145:151-177.

Darcy, H. 1856. Les Fontaines Publiques de la Ville de Dijon. Dalmont.

Domenico, P. A., and F. W. Schwartz. 1990. Physical and chemical hydrogeology. Wiley.

Dullien, F. A. L. 1992. Porous media: Fluid transport and pore structure. 2nd edition. Academic Press.

Freeze, R. A., and J. A. Cherry. 1979. Groundwater. Prentice Hall. 604 p.

Gupte, S. K., and S. G. Advani 1997. Flow near the permeable boundary of a porous medium: An experimental investigation using LDA. Exp. Fluids. 22:408-422.

Güss, S. 1998. Oxygen uptake at the sediment-water interface simultaneously measured using a flux chamber method and microelectrodes: must a diffusive boundary layer exist? Est. Coast. Shelf Sci. 46:143-56.

Haldorsen, M. H. 1986. Simulator parameter assignment and the problem of scale in reservoir engineering, p. 293-340. *In* L.W. Lake and H. B. Caroll [eds.], Reservoir Characterization, Academic Press.

Hart, D.J., and W.S. Hammon III. 2002. Measurement of hydraulic conductivity and specific storage using the shipboard Manheim squeezer, p. 1-15. In Salisbury, M.H., M. Shinohara, C. Richter and others [eds.], Proceedings of the Ocean Drilling Program, Initial Reports, Volume 195.

Huettel, M., and G. Gust. 1992. Solute release mechanisms from confined sediment cores in stirred benthic chambers and flume flows. Mar. Ecol. Prog. Ser. 82:187-197.

———, W. Ziebis, and S. Forster. 1996. Flow-induced uptake of particulate matter in permeable sediments. Limnol. Oceanogr. 42(2):309-322.

———, ———, ———, and G.W. Luther III. 1998. Advective transport affecting metal and nutrient distributions and interfacial fluxes in permeable sediments. Geochim. Cosmochim. Acta 62:613-631.

Klute, A. 1965. Laboratory measurement of hydraulic conductivity of saturated soil, p. 210-221. *In* C. A. Black [ed.], Methods of soil analysis, Part I: Physical and mineralogical methods, American Society of Agronomy, and Soil Science Society of America.

——— and C. Dirksen. 1986. Hydraulic conductivity and diffusivity: Laboratory methods, p. 687-734. *In* A. Klute [ed.], Methods of soil analysis. Part 1. 2nd edition, Agron. Monogr. 9. ASA and SSSA.

Le Loc'h, G. 1987. Étude de la composition des permeabilités par des methódes variatiuonelles, PhD thesis, Paris School of Mines.

Liu, S., T. -C. Jim Yeh, and R. Gardiner. 2002. Effectiveness of hydraulic tomography: Sandbox experiments. Wat. Resour. Res. 38(4):5.1-5.9.

Lohse, L., E. H. G. Epping, W. Helder, and W. van Raaphorst. 1996. Oxygen pore water profiles in continental shelf sediments of the north sea—Turbulent versus molecular diffusion. Mar. Ecol. Prog. Ser. 145(1-3):63-75.

Maulé, C. P., T. A. Fonstad, S. K. Vanapalli, and G. Majumdar. 2000. Hydraulic conductivity reduction due to ponded hog manure. Can. J. Agric. Eng. 42(4):157-163.

Miller, J. C., and J. N. Miller. 1984. Statistics for analytical chemistry (Ellis Horwood series in analytical chemistry). 202 pp.

Olson, M. S., F. D. Tillman Jr, J. -W. Choi, and J. A. Smith. 2001. Comparison of three techniques to measure unsaturated-zone air permeability at Picatinny Arsenal, NJ. J. Contam. Hydrol. 53:1-19.

Phillips, O. M. 1991. Flow and reaction in permeable rocks. Cambridge Univ. Press.

Press, W. H., S. A. Teukosky, W. T. Vetterling, and B. P. Flannery. 1986. Numerical recipes. Cambridge Univ. Press. 848 p.

Reimers, C. E., and others. 2004. In situ measurements of advective solute transport in permeable shelf sands. Cont. Shelf Res. 24:183-201.

Renard, Ph., G. Le Loc'h, E. Ledoux, G. De Marsily, and R. Mackay. 2000. A fast algorithm for the estimation of the equivalent hydraulic conductivity of heterogeneous media. Water Resour. Res. 36(12):3567-3580.

——— and G. de Marsily. 1997. Calculating equivalent permeability: a review. Adv. Water Resourc. 20(5-6):253-278.

Rocha, C. 1998. Rhythmic ammonium regeneration and flushing in intertidal sediments of the Sado estuary. Limnol. Oceanogr. 43(5):823-831.

———. 2000. Density-driven convection during flooding of warm, permeable intertidal sediments: the ecological importance of the convective turnover pump. J. Sea Res. 43:1-14.

Rowsell, J. G., M. H. Miller, and P. H. Groenbelt. 1985. Self-sealing of earthen liquid manure ponds. II. Rate and mechanisms of sealing. J. Environ. Quality 14(4):539-543.

Shum, K. T., and B. Sundby 1996. Organic matter processing in continental shelf sediments—the subtidal pump revisited. Mar. Chem. 53:81-87.

Svensson, U., and Rahm, L. 1991. Toward a mathematical model of oxygen transfer to and within bottom sediments. J. Geophys. Res. 96:2777-2783.

Thibodeaux, J. L., and J. O. Boyle 1987. Bed-form generated convective transport in bottom sediment. Nature 350:53-55.

Tindall, J. A., and J. R. Kunkel. 1999. Unsaturated zone hydrology for scientists and engineers. Prentice Hall.

Troyer, W., and J. Skopp. 2002. Rapid water flow instrumentation. Soil. Sci. Soc. Am. J. 67:107-111.

Vogel, H. -J., and K. Roth. 2003. Moving through scales of flow and transport in soil. J. Hydrol. 272:95-106.

Wang, Z., J. Feyen, M. T. van Genuchten, D. R. Nielsen. 1998. Air entrapment effects on infiltration rate and flow instability. Wat. Resour. Res. 34(2):213-222.

Webb, J. E., and J. L. Theodor. 1968. Irrigation of submerged marine sands through wave action. Nature 220: 682-683.

Webster, I. T., S. J. Norquay, F. C. Ross, and R. A. Wooding. 1996. Solute exchange by convection within estuarine sediments. Est. Coast. Shelf Sci. 42:171-183.

Zlotnik, V. A., and V. L. McGuire. 1998. Multi-level slug tests in highly permeable formations: 2. Hydraulic conductivity identification, method verification, and field applications. J. Hydrol. 204:283-296.

Submitted 17 February 2004
Revised 20 July 2004
Accepted 20 October 2004